Available online at www.sciencedirect.com
SCIENCE DIRECT®
Journal of Membrane Science 239 (2004) 119–128
journal of MEMBRANE SCIENCE
www.elsevier.com/locate/memsci

Role of membrane surface in concentration polarization at cation exchange membranes

R. Ibanez[1], D.F. Stamatialis, M. Wessling*

Membrane Technology Group, Faculty of Science and Technology, University of Twente, P.O. Box 217, NL-7500 AE Enschede, The Netherlands

Received 8 May 2003; received in revised form 30 November 2003; accepted 18 December 2003

Available online 22 April 2004

Abstract

Cation exchange membranes made of blends of sulphonated polyetherether ketone (S-PEEK) and poly(ether sulphone) (PES) were thoroughly characterized with respect to their concentration polarization properties. Current–voltage curves and chronopotentiometry reveal some extent of membrane heterogeneity. Membranes cast on a glass plate and dried in air are characterized and the current–voltage curves are determined for each of the two membrane sides (glass side contact and air side contact). Detailed analysis of the plateau length at the limiting current density reveals differences as the orientation of the membrane towards the feed is changed. The plateau length of the air side of the membrane always shows larger values compared to the glass side. Moreover, we discovered that the plateau length of the glass side remains constant whereas the air side value increases over a period more than 500 h approaching a quasi-equilibrium value, asymptotically. These data are the first ones suggesting an influence of orientation on the concentration polarization behavior as well as relaxation phenomena occurring in cation exchange membranes. The paper discusses strategies to gain new fundamental insight in the relationship between membrane morphology and transport properties by for instance microstructuring the surface.

Keywords: Cation exchange membranes; Concentration polarization current; Electro-convection; Surface heterogeneity; Microstructuring

1. Introduction

Concentration polarization hampers the optimization of membrane processes severely. Due to the imbalance of hydrodynamic boundary layer resistance and membrane resistance—the membrane resistance becomes of the order of magnitude or even smaller than the hydrodynamic boundary layer resistance—concentration gradients evolve in the feed at the membrane surface. In its most prominent form, concentration polarization is observed by the fact that the transmembrane flux does not increase with increasing driving force and reaches a limiting flux. In electrodialysis with monopolar membranes, this limiting flux is called the limiting current density with the voltage drop across the membrane as a measure for the driving force [1–3]. In contrast to membrane processes such as pervaporation, vapor permeation and ultrafiltration, in electrodialysis there appears a remarkable phenomenon if one proceeds to increase the driving force: an overlimiting current sets in. Fig. 1 visualizes the characteristic features of such a current–voltage curve. Three regions can be distinguished:

1. a linear part giving the ohmic resistance of the solution and the membrane between the reference (measurement) electrodes;
2. a plateau region caused by ion-depletion in the hydrodynamic boundary layer and being called the limiting current; and
3. a region in which transport sets in at higher driving forces.

Decades of research focussed on the transition between the first and the second region [4–15], the deviation from ohmic behavior and the appearance of current limitation due to increasing resistance in the hydrodynamic boundary layer. We consider this phenomenon as well understood with many studies confirming the overall mass transport considerations. Still, the influence of membrane heterogeneity on the mag-

* Corresponding author. Tel.: +31-53-489-2951; fax: +31-53-489-4611.
E-mail address: m.wessling@utwente.nl (M. Wessling).
[1] Present address: Department of Engineering Chemistry and Inorganic Chemistry, University of Cantabria, Avda. Los Castros, s/n, 39005 Santander, Spain.

0376-7388/$ – see front matter © 2004 Elsevier B.V. All rights reserved.
doi:10.1016/j.memsci.2003.12.032

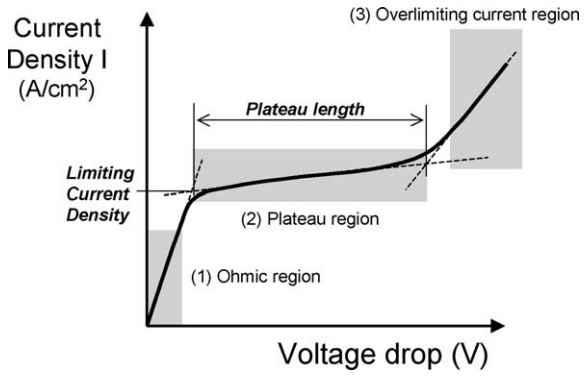

Fig. 1. Schematic drawing of a typical voltage–current curve of a monopolar ion exchange membrane indicating three typical regions characteristic to the phenomenon of concentration polarization, the limiting current density and the plateau length.

nitude of the limiting current density attracts experimental and theoretical attention.

Region 3, the onset of current at high driving forces or voltage drop has been puzzling and intriguing for as long as the phenomenon of concentration polarization in electrodialysis exists. For a long time, region 3 was attributed to the generation of acid or base by water splitting [16]. This hypothesis was based on experimental evidence of pH changes observed in desalination using anion exchange membranes. Later, however, the absence of water splitting at cation exchange membranes diluted the argument of water splitting in the overlimiting current region. Detailed mass balances for cation and anion exchange membranes verified that the majority of ion transport occurs through a different mechanism [17].

A group of Israeli scientists around I. Rubinstein explored the physical origin of enhanced transport in the overlimiting current region [18–24]. In particular, Rubinstein elaborates in detail on the theory of electro-convection as a phenomenon that destabilizes the hydrodynamic boundary layer. Electro-convection is a non-gravitational convection caused by the interaction of a self-consistent electric field with the corresponding electric charge, either in macroscopic quasi-electro-neutral domains of electrolyte ("bulk electro-convection") or in the quasi-equilibrium or non-equilibrium electric double layer ("electro-osmotically induced convection"). Theoretically heterogeneity of the membrane surface is not crucial for electro-convection, which may occur at a perfectly homogenous membrane due to electro-convective instability of quiescent concentration polarization. However, the onset of instability may be precipitated by the non-uniformity of the membrane surface, either geometrical (undulation on the right scale) or morphological (conductive heterogeneity).

Very little is known about region 2, the plateau length in particular. Rubinstein predicts the length of the plateau to decrease if one would be able experimentally to imprint a surface undulation. Strong experimental evidence exists indicating that the plateau length decreases with increasing stokes radius of the ion transported [25]. Some experimental evidence can be found in the above-mentioned references that the length of the plateau shows differences for different membranes. To the best of our knowledge however, no systematic approach exists supporting the hypothesis that the length of the plateau is related to the surface morphology of the ion exchange membrane, i.e. the distribution of more and less conductive phases. Rubinstein poses the question whether "one can influence polarization and local mixing of the boundary layer by designed inhomogeneity" [10]?

This paper aims: (a) to extend the knowledge on the transport behavior of microheterogeneous blended ion exchange membranes made of sulphonated polyetherether ketone (S-PEEK) and polyethersulfone [26] with respect to concentration polarization, (b) report detailed experiments and new results addressing the fundamental question on the extent of the plateau in region 2, and finally (c) reflect on research strategies to better understand the phenomenon of electro-convection.

2. Experimental

2.1. Membrane formation and characterization

Cation permeable membranes (CEM) have been cast from solutions of sulphonated poly(ether ether ketone) (S-PEEK) and neutral poly(ether sulphone) (PES) in a solvent (*n*-methyl pyrrolidine, short: NMP). PEEK 450 PF (Victrex) has been randomly sulphonated with sulphuric acid (Merck, analytical grade) according to the procedure described in references [26–28]. Dense membranes are prepared by solvent evaporation according to the following procedure: the solvent is added to the base polymers in the desired weight ratio, ranging from 50 to 100 wt.% S-PEEK in a blend with PES; the final concentration of polymer is 20 wt.% in the casting solution. At room temperature, the viscous solution is cast on a glass plate with a casting knife having a fixed opening of 0.50 mm. The membrane is dried following the temperature program described in [26]. When the membrane is dry, it is removed from the glass plate by immersion in a sodium chloride solution (0.5 mol/l). During further storage in this solution, the material is transferred into the sodium-form, i.e. the proton of the fixed sulphonic acid group is exchanged with a sodium ion.

Two sets of S-PEEK/PES CEM have been used in this study. The first set had been cast in a previous study [26] and kept dry for a long period. These membranes, blends from 50 to 100% S-PEEK percentage, were coded ACM + number (indicating Aged Cationic Membranes + S-PEEK percentage in blend). The air and glass side of the membranes was not identified in this set. The sides are assigned bottom (b) and top (t). The second set was cast during this study. These membranes, blends from 50 to 100% S-PEEK percentage, were coded NCM + number (indicating New Cationic Membranes + S-PEEK percentage in blend). The

air and glass side of the membranes was explicitly identified in this set.

The ion exchange capacity, water uptake, electrical resistance and degree of sulphonation have been determined in the NCM following the procedures described in [26,29] that were used previously to characterize the ACM.

2.2. Current–voltage and chronopotentiometric curves

Current–voltage curves have been determined with a set-up comprising of a Plexiglas membrane cell, which consists of six separate compartments [17]. The two outer compartments contain the working electrodes, i.e. a platinized titanium anode and a stainless steel cathode. The central membrane in the cell is the membrane under investigation, the other membranes are auxiliary membranes. The area of the auxiliary membranes is 23.8 cm^2 and the area of the membrane under investigation is 3.14 cm^2. All experiments were performed at 25 °C. (More information about the experimental set-up and the membrane cell can be obtained in [15,17].) Tokuyama Soda Inc., Japan, has supplied the auxiliary CEM and AEM used in the experiments. They are reinforced, standard grade membranes for general concentration or desalination purposes [30]. The central membrane is the S-PEEK/PES blend CEM under investigation. A CEM is positioned next to the anode compartment to prevent chloride transport to the anode thereby avoiding the production of chlorine gas at this electrode. In the electrode compartments, 0.5 M Na_2SO_4 (Merck, analytical grade) was used. In the other four compartments, NaCl (Merck, analytical grade) solutions were used. The concentration in the second and fifth compartment was 0.5 M, the concentration in the third and fourth compartment (adjacent to the test membrane) ranged from 0.1 to 0.5 M.

Current–voltage curves were determined by a stepwise increase of the current density through the cell. After an increase in the current, the system was allowed to reach steady state for some time (more than 3 min) after which the voltage across the test membrane was measured, followed by the next current increase. The obtained combinations of current density and membrane voltage drop gave the experimental current–voltage curve.

Chronopotentiometric curves have also been obtained in this study using the same experimental set-up described above [15]. The experiment started with no current applied and since the solutions on either side of the membrane are equal, the voltage drop remains zero. At a given time, a fixed value of the current density was applied to the membrane cell and the voltage drop across the membrane was measured as a function of time.

Atomic force microscopy (AFM) has been used to determine surface characteristics of the S-PEEK/PES blends. The AFM measurements have been performed using a Nanoscope IIIa (Digital Instruments). The instrument was equipped with a Silicon tip (nanosensor) and operated in tapping mode. The scanning rate was 1.4 Hz.

Table 1
Ion exchange capacity and water uptake properties of S-PEEK/PES blends

$W_{S\text{-}PEEK}$ (%)	Ion exchange capacity (mol/g)		Water uptake (g/g_{dry})	
	ACM[a]	NCM[b]	ACM[a]	NCM[b]
100	2.14	1.90	0.45	0.43
90	1.80	1.70	0.35	0.36
80	1.65	1.60	0.30	0.28
70	1.48	1.36	0.24	0.24
60	1.20	1.21	0.19	0.17
50	1.00	0.98	0.15	0.13

[a] Data reported from [26]. S-PEEK sulphonation degree 0.70 mol/mol.
[b] Data obtained in this work. S-PEEK sulphonation degree 0.65 mol/mol.

3. Results and discussion

3.1. Membrane characterization

Two sets of membranes have been used in this work: aged cationic membranes (coded ACM) and new cationic membranes (coded NCM). Both sets have been cast according to the procedure described in Section 2.1. A complete characterization of the aged membranes, including resistance, ionic conductivity, ionic exchange capacity (IEC), water uptake, fixed charge density, etc., can be found in [26]. A comparison of the ion exchange capacity and water uptake between ACM and NCM is shown in Table 1. Ionic conductivity has also been measured in the new cast S-PEEK/PES blends to assure that the membrane characteristics were the same. Fig. 2 shows the specific conductivity values corresponding to aged and new cast membranes using NaCl 0.5 mol/l. The conductivity values shown in the figure indicate that CEM from solutions of S-PEEK and PES using NMP as solvent are very reproducible. Conductivity values of the new membranes are slightly smaller than the aged membranes for the same blend ratio. This must be attributed to the different degree of sulphonation obtained in the S-PEEK used in each set: 0.70 mol/mol in the S-PEEK used in the aged blends [26] and 0.65 mol/mol in the S-PEEK used in the new blends.

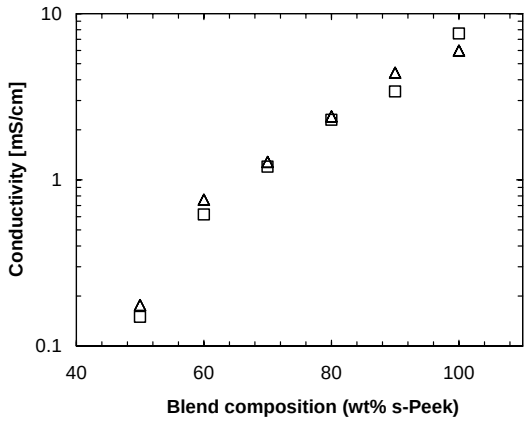

Fig. 2. Ion conductivity measured in NaCl (0.5 mol/l) as a function of the S-PEEK content in the S-PEEK/PES blends for aged (triangles) and new (squares) membranes.

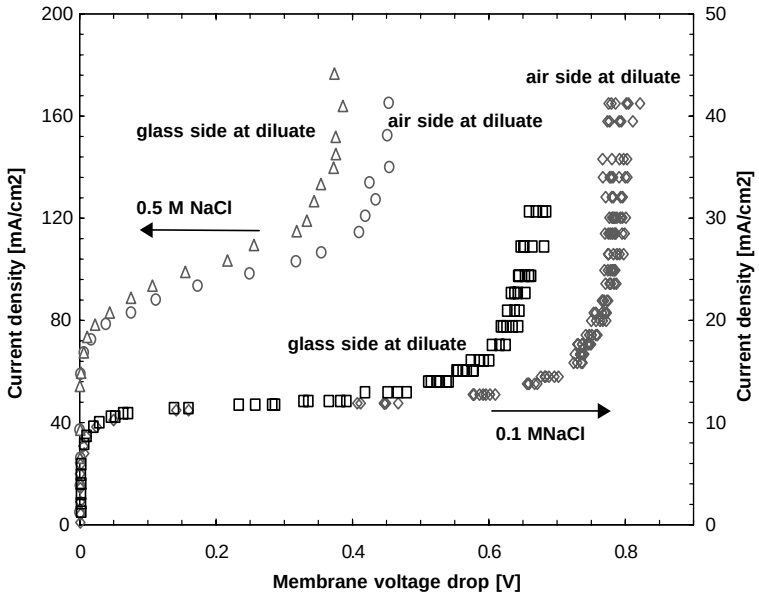

Fig. 3. Current–voltage curves of NC membranes (100% S-PEEK) in 0.5 and 0.1 M NaCl. The preparation side of the membrane towards the diluate is also indicated.

3.2. Limiting current density

Current–voltage curves were determined using both 0.5 and 0.1 M NaCl solutions and the set up previously described. The limiting current density was determined for both sets of membranes, aged (ACM) as well as new cation exchange membranes (NCM), in both orientations (bottom/top and air/glass side). Unless other reported, the membranes are characterized after an equilibration period of at least 12 h. This period is sufficient to obtain reproducible permselectivity and ohmic resistances. The stepwise increase of the current density through the cell was pursued until the overlimiting region was measured. Fig. 3 shows the current–voltage curves for NCM membranes at the two feed concentrations corrected for the ohmic resistance of the membrane and salt solution between the measurement electrodes. Clearly, the limiting current densities are visible as well at the plateaus and the overlimiting currents. Surprisingly, differences in the curves, especially the plateau length as a function of the orientation towards the feed solutions, are clearly detectable. More details of this remarkable observation will be discussed in the second part of this paper.

Table 2 summarizes the limiting current densities for all membranes and verifies that the value of the limiting current

Table 2
Limiting current density for S-PEEK/PES blends, in NaCl solutions

Code	Position[a]	Limiting current density (mA/cm^2)		Code	Position	Limiting current density (mA/cm^2)	
		0.5 M NaCl	0.1 M NaCl			0.5 M NaCl	0.1 M NaCl
ACM100	t	80.1 ± 4.0	10.2 ± 0.5	NCM100	Air	77.6 ± 3.8	10.4 ± 0.5
	b	76.6 ± 3.8	10.8 ± 0.5		Glass	80.3 ± 4.0	10.2 ± 0.5
ACM90	t	83.7 ± 4.1	10.6 ± 0.5	NCM90	Air	76.9 ± 3.8	9.5 ± 0.4
	b	73.1 ± 3.6	10.4 ± 0.5		Glass	75.4 ± 3.7	9.0 ± 0.4
ACM80	t	80.3 ± 4.0	10.5 ± 0.5	NCM80	Air	80.8 ± 4.1	9.7 ± 0.4
	b	78.4 ± 3.9	10.8 ± 0.5		Glass	77.3 ± 3.8	9.7 ± 0.4
ACM70	t	72.2 ± 3.6	10.2 ± 0.5	NCM70	Air	75.2 ± 3.7	9.8 ± 0.4
	b	72.3 ± 3.6	10.6 ± 0.5		Glass	78.7 ± 3.9	10.1 ± 0.5
ACM60	t	75.0 ± 3.7	10.2 ± 0.5	NCM60	Air	77.9 ± 3.8	9.1 ± 0.4
	b	73.0 ± 3.6	10.1 ± 0.5		Glass	81.3 ± 4.2	9.2 ± 0.4
ACM50	t	77.5 ± 3.8	9.9 ± 0.4	NCM50	Air	–	–
	b	80.0 ± 4.0	10.3 ± 0.5		Glass	–	–

[a] t and b are used to differentiate both sides of a membrane, the subscript 't' is used for the surface in which the membrane name is written (suppose to be air side of the membrane). The subscript 'b' is used for the other surface (suppose to be glass side).

density increases with increasing bulk solution concentration as expecting according to:

$$i_{\lim} = \frac{Fc^{b}D}{\delta(\bar{t}_i - t_i)} \quad (1)$$

where $i_{\lim}$ is the limiting current density, c^{b} is the bulk solution concentration, D is the diffusion coefficient, F is the Faraday constant, $\bar{t}_i$ is the transport number in the membrane, t_i is the transport number in the solution and δ is the boundary layer thickness. At a constant bulk solution concentration, the limiting current density is hardly affected by the blend composition (percentage of S-PEEK in the blend). This is valid for both sets of membranes (ACM and NCM) as well as for the different orientations of the membranes (t versus b, or air side versus glass side). The only material property entering the equation for the limiting current density is the transport number of the membrane. Considering the small variations in the co-ion transport numbers reported for such membranes (it varies between 0.01 and 0.02 [26]) with respect to the average transport number in the laminar boundary layer (0.39 for 0.1 M NaCl solution), we do not expect any effect of blend composition on the limiting current density based on permselectivity arguments. The transport number in the membrane can be therefore be assumed to equal $\bar{t}_i = 1$. Nonetheless, some scatter in the value can be observed which we relate later to the surface structure of the blend membranes. It has been suggested that the ionic conductance through the membrane is not uniform. In the conducting regions, the local current would be larger than the measured average value and thus lead to a lower overall limiting current. To quantify the heterogeneity of the surfaces remains a challenge in particular for the microheterogeneous blend membranes: phase separated domains of the conducting and inert phase may be in the micro and submicrometer range requiring an analysis method with sufficient resolution.

3.3. Chronopotentiometry

Chronopotentiometic measurements reveal additional details on the polarization characteristics of the S-PEEK/PES blends membranes. This technique has successfully been applied to determine a reduced permeable area with ion exchange membranes. As explained in the previous sections, when an electric current is applied to a system containing an ion exchange membrane, concentration polarization arises. The transient decrease of the salt concentration at the membrane–solution interface can be followed by measuring the voltage drop across the membrane as a function of time. Eq. (2) describes the time-dependent concentration at the membrane surface for a system comprising of a homogeneous ion selective interface in contact with a univalent electrolyte solution in absence of a supporting electrolyte and without any form of convection:

$$c(0,t) = c_0 - \frac{2i}{zFD}(\bar{t}_i - t_i)\sqrt{\frac{Dt}{\pi}} \quad (2)$$

where z is the electrochemical valence. At a characteristic time, τ, called the transition time, this interface concentration reaches zero. The transition time as a function of applied current density can be derived from Eq. (2) and it is given by

$$\tau = \frac{\pi D}{4}\left(\frac{c_0 zF}{\bar{t}_i - t_i}\right)\frac{1}{i^2} \quad (3)$$

Eq. (3) shows that the transition time is proportional to the inverse of the current density squared and that the transition time increases when the membrane transport number decrease, i.e. when the membrane is less permselective.

The presence of overlimiting currents for the S-PEEK/PES blends membranes has been demonstrated in the previous sections by stepwise increasing the current density and measuring the static potential drop across the membrane. Chronopotentiometry gives the dynamics by which this equilibrium is reached. The typical example of a chronopotentiometric curve measured in a commercial CMX membrane is fully explained elsewhere [15,31]. In these sections, the results of the chronopotentiometric curves corresponding to S-PEEK/PES blends are discussed. Fig. 4 shows a characteristic set of chronopotentiometric curves measured at different applied current densities with S-PEEK/PES blends using 0.1 M NaCl. At a current density below the limiting current, no sudden increase in voltage drop is measured in contrast to current densities above the limiting value. Also, the curves below the limiting current density are not characterized by a transition time because the concentration at the membrane–solution surface does not reach zero. Above the limiting current density, characteristic transition times predicted by Eq. (3) are found. After the sharp voltage rise at the transition time, the voltage drop levels off and a quasi-steady state is reached showing fluctuations around an average value. This is in agreement with the considerable scatter in data points in the overlimiting region of

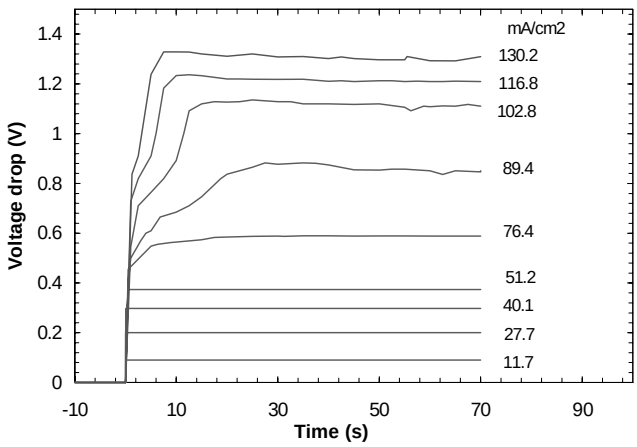

Fig. 4. Typical chonopotentimetric curves at various current densities in 0.1 M NaCl.

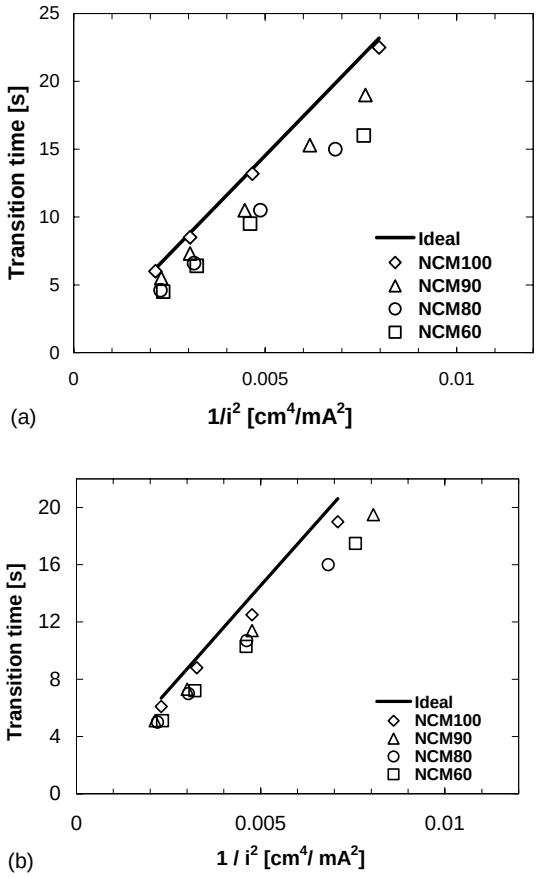

Fig. 5. Comparison between experimental transition times and ideal transition times (solid lines) for the S-PEEK/PES membranes: (a) glass side at diluate; (b) air side at diluate.

a current–voltage curve as shown in Fig. 3. For the measurement system used, Krol et al. [15] demonstrated that these fluctuations are not a result of a forced convection or gravitational convection.

Fig. 5a and b shows the transition time as a function of the inverse of the current density squared for NCM for the air side and glass side: a linear relationship between the transition time and the inverse current density squared is obtained. Increasing applied current density reduces the transition time since the ion flux depleting the interface increases with increasing current density. Fig. 5a and b also shows the predicted transition time according to Eq. (3). For the calculation, a NaCl diffusion coefficient of 1.48×10^{-9} m^2/s and a Na^+ solution transport number of 0.39 were used for the 0.1 M NaCl solution. The experimentally determined transition times are slightly smaller than the transition times calculated for an ideally permselective and homogeneous membrane. According to former studies [15], any non-ideal behavior of a real system, such as a reduced permselectivity, consumption of non-faradaic currents for charging of double layers and the onset of natural convection, can only result in transition times higher than predicted by theory. Hence, transition times lower than the values calculated for an ideally permselective membrane can only be due to a reduction in available membrane area for ion conductance. A reduced permeable membrane area corresponds to a locally higher current density at those points where the membrane is conductive. This causes a faster depletion of salt near the membrane, i.e. a lower transition time is measured compared to the situation where the complete membrane area is available for ion conductance. This behavior is in accordance to earlier observations by other researchers working with commercial CEM like Neosepta CMX (Tokuyama Soda Co.), Selemion CMV (Asahi Glass Co.), Heterogeneous CEM by Hanguk Jungsoo Co. [14], Neosepta AEM (Tokuyama Soda Co.) [15] and laboratory made sulphonated polysulphone membranes [12].

The reduced experimental transition times in Fig. 5a and b can be used to extract further information on the morphology of the blend membranes. The 100% S-PEEK membrane shows a behavior closer to that expected for an ideal membrane in the same conditions. Still, experimentally determined transition times for 100% S-PEEK membranes are slightly smaller than the transition times calculated for an ideally permselective membrane (mainly when the air side of the membrane is considered). Transition times are even smaller as S-PEEK percentage in blends decreases mainly when the glass side of the membrane is used. Considering that the effective current density increases as the membrane surface becomes more heterogeneous, Eq. (3) indicates that the effective conductive surface area can be estimated by the square root of the ratio of the ideally calculated slope and the real slope in Fig. 5. Doing so, one can estimate that for most of the membranes, independent of the blend composition, an effective conducting surface area of 90% exists. If indeed region 2, in particular the plateau length, is supposed to be affected by the surface heterogeneity, the differences in heterogeneity for the various blends (suggested by the reduced transition times) is not significant to establish a clear relationship between blend composition and plateau length.

3.4. Plateau length at limiting current density

Frequently, publications on the characteristics of monopolar ion-exchange membrane state that the current–voltage curves must be measured at well-equilibrated membranes. Experience says that at least 12 h equilibration time is required to obtain reproducible electrical resistance or permselectiviy values. Initially, we assumed this criterion to hold also for the analysis of the polarization behavior and the onset of the overlimiting current. At the two different salt concentrations, we determined the complete current–voltage curves of all membranes and all orientations. From the intersection points depicted in Fig. 1, the length of the plateau could be identified. Errors for the plateau length can be estimated from the linear regressions performed in regions 1 and 3. Figs. 6 and 7 show the plateau length, expressed as the increase in voltage needed to reach the overlimiting current density, for ACM and NCM, respectively. The figures do not show a straightforward experimental trend between

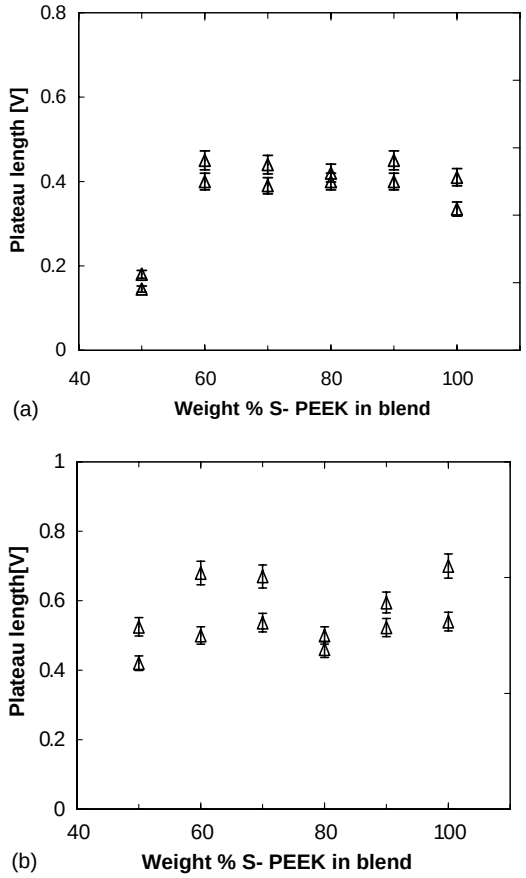

Fig. 6. Plateau length in current–voltage curves for aged S-PEEK/PES blends membranes: (a) 0.5 M NaCl; (b) 0.1 NaCl.

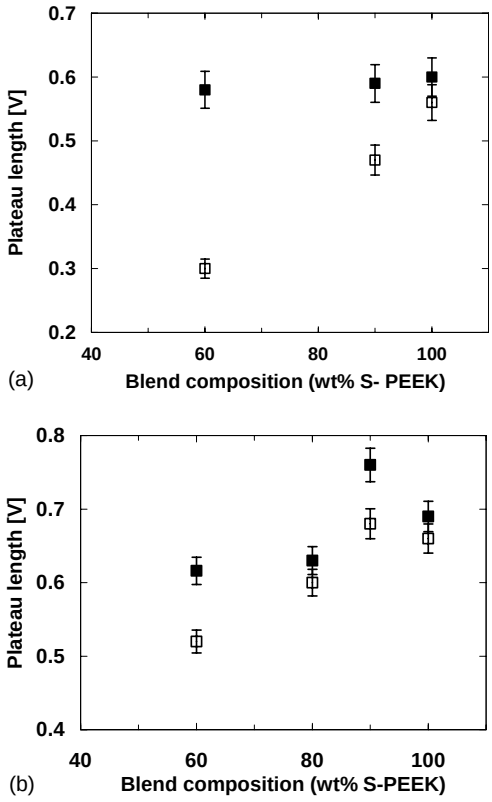

Fig. 7. Plateau length in current–voltage curves for new S-PEEK/PES blends membranes: (a) 0.5 M NaCl; (b) 0.1 M NaCl. The filled symbols denote membrane with air side at diluate and the open symbols denote membrane with glass side at diluate.

blend composition and plateau length. However, the figures allow extraction of yet unknown observations.

For the aged membranes, we could not distinguish an air or glass side. Fig. 6 allows only one conclusion: for some blend compositions there exists a difference in the plateau length depending on the orientation of the membrane. Fig. 7, however, allows the extraction of more information since glass and air side are well known. For membranes with the "glass side" facing the diluate, the plateau is systematically shorter than the "air side". Most prominent is this difference at higher salt concentrations in the feed solution and at low weight fractions of S-PEEK blended into PES. To the best of our knowledge, these data are the first reporting that one single membrane may show different polarization characteristics for the two sides of a membrane.

Rubinsteins theoretical framework reveals that membrane inhomogeneity as well as a surface undulation may effect the length of the plateau. Detailed AFM analysis in tapping mode was performed to determine any surface roughness (read undulation), however, surface roughnesses determined on a 10 μm × 10 μm area as well as 50 μm × 50 μm area revealed a low surface roughness in the nanometer range (spanning from 2 to 8 nm) and no significant difference between the two sides. We, therefore, exclude surface roughness to influence the plateau length. However, it is not unlikely that the surface properties, i.e. segregation of ion-exchange and neutral polymer phases, of the blend membranes is strongly affected by the surface at which the film dries against. Two mechanism may be responsible for the differences at the two surfaces of the film: (i) the surface energies are different with the polymer solution exposed to the air and to the glass plate. Of the two polymers one could prefer the contact with the glass plate, the other with the air phase; (ii) in the film, a concentration gradient of the solvent in the drying film is present. The slow evaporation allows for demixing of the polymer phases on a micro-scale, different for different solvent concentrations. It is known from literature that conditioning of ion exchange membranes can affect their electro-transport properties [32].

Figs. 6 and 7 leave open the question whether there exists a clear relationship between the blend composition and the polarization behavior, in particular the plateau length. The existence of differences in transport behavior of the different membrane sides is evident, but, a relationship to the membrane composition appears far-fetched. Nonetheless, we think that there exists evidence that such a relationship may be established. Only by coincidence we discovered that the plateau length is not an equilibrium property of

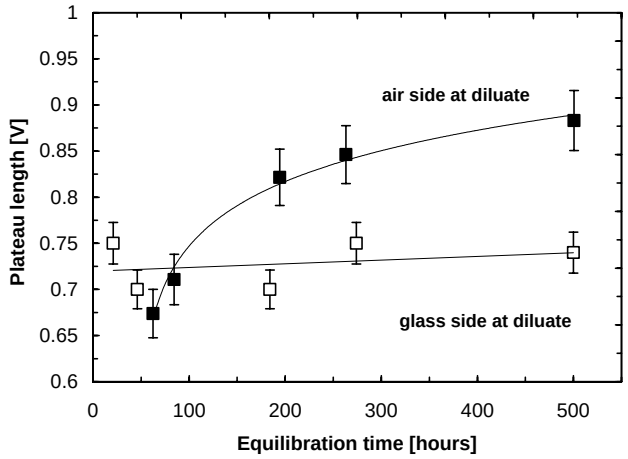

Fig. 8. Plateau length in current–voltage curves (0.1 M NaCl) vs. equilibration time for 100% S-PEEK membrane. The filled symbols denote membrane with air side at diluate and the open symbols denote membrane with glass side at diluate.

the membranes. During the reproduction of current–voltage curves, differences in curves were discovered with respect to the plateau length for air side of the membrane: whereas the plateau length of the glass side remained constant. We followed this behavior in time over a period of about 500 h. Fig. 8 shows the plateau length as a function of the equilibration time. A surprising observation evolves: the plateau length for the air side of the membrane develops towards larger voltage drops. Initially, insignificant differences between glass and air side develop into experimentally significant values over extended time periods. Hence, we hypothesize today that there may be differences in surface morphology, but also that this surface morphology may have a transient character. Any further interpretation, such as reorganization of hydrophilic and hydrophobic domains, remains merely speculation.

The following experiments give further support to the picture of differences in surface morphology and their effect on the onset of the overlimiting current. New blend membranes of S-PEEK and PES were first characterized with respect to their plateau length and the characteristic differences were observed again. After this characterization, the membranes were incubated with polyethylenimine (PEI), a poly-cation following the protocol of [33]. Due to strong electrostatic interaction between the cation exchange membrane and the poly-cation, the membrane surface was covered with a thin layer of PEI. Subsequent current–voltage curve analysis revealed coinciding curves for the different sides facing the feed solution. Apparently, the PEI coating screens the differences in surface morphology completely. However the coating is not strong enough to surpress electro-convection completely as Rubinstein reports for PVA coated cation exchange membranes [24]. Currently, we perform further detailed studies on transport number, concentration polarization behavior and surface potential of these sandwiched composite membranes.

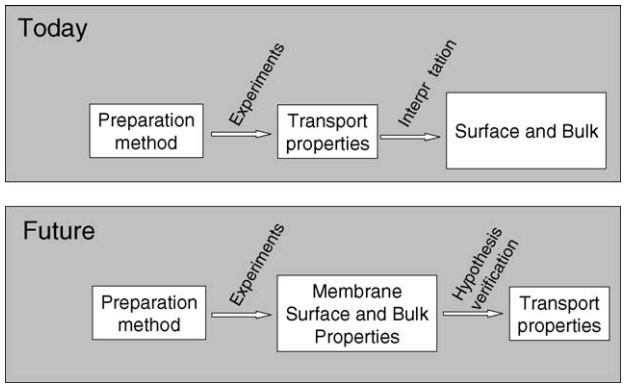

Fig. 9. Schematic visualization of current research strategies and proposed future approaches.

4. Reflections and outlook

Considering the current and previous work published in various journals, one must conclude that the research strategy often follows a pattern visualized in Fig. 9. Commercial membranes are taken and compared, or they are modified by a simple coating, or the ion exchange capacity is varied and the transport properties are measured. Deviations from models are interpreted in terms of membrane morphology. Only little effort has been taken until today to verify the interpretations since the surface heterogeneity is difficult to assess experimentally.

To gain new fundamental knowledge and strong proof of the theory of electro-convection, we propose the following approach: spend significant resources on the precise structuring of the interface of the ion-exchange membranes according to an hypothesis, perform thorough characterization of the surface morphology and finally verify the hypothesis by transport measurements.

To illustrate this methodology, we performed initial experiments on imprinting an undulation on a cation exchange membrane. Such membranes can be prepared by casting the solution on a silicon machined master wafer having patterns etched into the surface by photolithography. Using masters of different depth one can systematically vary the undulation pattern on the membrane. With increasing depth, ranging from 0 to 70 μm, the plateau length decreases by up to 20% whereas the limiting current density remains constant. Rubinsteins theory of electro-convection predicts a shortening of the plateau length with the introduction of a wavy surface, as well. These preliminary experiments do not claim to proof the theory, however, they support the idea that we can influence polarization and local mixing of the boundary layer by designed inhomogeneity.

Acknowledgements

This work was supported by a grant from the “Movilidad del profesorado universitario” Program of the Spanish

Nomenclature

c	concentration (mol/m^3)
D	diffusion coefficient (m^2/s)
F	Faraday constant (96,485 A s/mol)
i	current density (A/m^2)
t	time (s)
t_i	transport number in solution (–)
$\bar{t}_i$	transport number in membrane (–)
z	electrochemical valence (–)

Greek letters

δ	boundary layer thickness (m)
τ	transition time (s)

Superscript

b	bulk solution

Subscripts

lim	limiting
0	initial

Research Department. We thank I. Rubinstein and Y. Oren for inspiring discussions, and O. Krupenko and J. Balster for independent verification of current–voltage curves.

References

[1] N.W. Rosenberg, C.E. Tirell, Limiting currents in membrane cells, Ind. Eng. Chem. 49 (1957) 780–784.
[2] K.S. Spiegel, Polarization at ion exchange membrane solution interfaces, Desalination 9 (1971) 367–385.
[3] V.K. Indusekhar, P. Meares, The effect of the diffusion layer on the ionic current from a solution into an ion-exchange membrane, in: D.B. Spalding (Ed.), Physicochemical Hydrodynamics II, Advance Publications, London, 1977, pp. 1031–1043.
[4] V.M. Barragán, C. Ruíz Bauzá, Current–voltage curves for a cation-exchange membrane in methanol–water electrolyte solutions, Interface Sci. 247 (2002) 138–148.
[5] V.M. Barragán, C. Ruíz-Bauzá, Current–voltage curves for ion-exchange membranes: a method for determining the limiting current density, J. Colloid Interface Sci. 205 (1998) 365–373.
[6] V.I. Zabolotsky, V.V. Nikonenko, N.D. Pismenkaya, E.V. Laktionov, M.Kh. Urtenov, H. Strathman, M. Wessling, G.H. Koops, Coupled transport phenomena in overlimiting current electrodialysis, Sep. Purif. Technol. 14 (1998) 255–267.
[7] V.M. Aguilera, S. Mafé, J.A. Manzanares, J. Pellicer, Current–voltage curves for ion exchange membranes. Contribution to the total potential drop, J. Membr. Sci. 61 (1991) 177–190.
[8] M. Taky, G. Pourcelly, F. Lebon, C. Gavach, Polarization phenomena at the interfaces between an electrolyte solution and an ion exchange membrane. Part I. Ion transfer with a cation exchange membrane, J. Electroanal. Chem. 336 (1992) 171–194.
[9] M. Taky, G. Pourcelly, C. Gavach, Polarization phenomena at the interfaces between an electrolyte solution and an ion exchange membrane. Part II. Ion transfer with an anion exchange membrane, J. Electroanal. Chem. 336 (1992) 195–212.
[10] I. Rubinstein, E. Staude, O. Kedem, Role of the membrane surface in concentration polarization at ion-exchange membrane, Desalination 69 (1988) 101–114.
[11] F. Maletzki, H.W. Rösler, E. Staude, Ion transfer across electrodialysis membranes in the overlimiting current range: stationary voltage current characteristics and current noise spectra under different conditions of free convection, J. Membr. Sci. 71 (1992) 105–115.
[12] H.W. Rösler, F. Maletzki, E. Staude, Ion transfer across electrodialysis membranes in the overlimiting current range: chronopotentiometric studies, J. Membr. Sci. 72 (1992) 171–179.
[13] I. Rubinstein, L. Shitlman, Voltage against current curves of cation exchange membranes, J. Chem. Soc. Faraday Trans. II 75 (1979) 231–246.
[14] J.H. Choi, S.H. Kim, S.H. Moon, Heterogeneity of ion-exchange membranes: the effects of membrane heterogeneity on transport properties, J. Colloid Interface Sci. 241 (2001) 120–126.
[15] J.J. Krol, M. Wessling, H. Strathmann, Chronopotentiometry and overlimiting ion transport through monopolar ion exchange membranes, J. Membr. Sci. 162 (1999) 155–164.
[16] R. Simons, The origin and elimination of water splitting in ion exchange membranes during water demineralisation by electrodoalysis, Desalination 28 (1979) 41–42.
[17] J.J. Krol, M. Wessling, H. Strathmann, Concentration polarization with monopolar ion exchange membranes: current–voltage curves and water dissociation, J. Membr. Sci. 162 (1999) 145–154.
[18] I. Rubinstein, L.A. Segel, Breakdown of a stationary solution to the Nerst–Planck–Poisson equations, J. Chem. Soc. Farady Trans. II 75 (1979) 936–940.
[19] I. Rubinstein, Effects of deviation from local electroneutrality upon electro-diffusional ionic transport across a cation-selective membrane, React. Polym. 2 (1984) 117–131.
[20] I. Rubinstein, Electroconvection at an electrically inhomogeneous permselective interface, Phys. Fluids A 3 (1991) 2301–2309.
[21] I. Rubinstein, F. Maletzki, Electroconvection at an electrically inhomogeneous permselective membrane surface, J. Chem. Soc. Faraday Trans. 87 (1991) 2079–2087.
[22] I. Rubinstein, B. Zaltzman, Electro-osmotically induced convection at a permselective membrane, Phys. Rev. E 62 (2000) 2238–2251.
[23] I. Rubinstein, B. Zaltzman, T. Pundik, Ion-exchange funneling in thin-film coating modification of heterogeneous electrodialysis membranes, Phys. Rev. E 65 (2002) 041507.
[24] I. Rubinstein, B. Zaltzman, J. Pretz, C. Linder, Experimental verification of the electro-osmotic mechanism of overlimiting conductance through a cation exchange electrodialysis membrane, Russ. J. Electrochem. 38 (2002) 853.
[25] J.-H. Choi, H.J. Lee, S.H. Moon, Effects of electrolytes on the transport phenomena in a cation exchange membrane, J. Colloid Interface Sci. 238 (2001) 188–195.
[26] F.G. Wilhelm, I.G.M. Pünt, N.F.A. van der Vergt, H. Strathmann, M. Wessling, Cation permeable membranes from blends of sulfonated poly(ether ether ketone) and poly(ether sulfone), J. Membr. Sci. 199 (2002) 167–176.
[27] V.L. Rao, Polyether sulphones, J. Macromol. Sci.: Rev. Macromol. Chem. Phys. C39 (1999) 655–711.
[28] W. Cui, J. Kernes, G. Eigenberger, Development and characterization of ion-exchange polymer blend membranes, Sep. Purif. Technol. 14 (1998) 145–154.
[29] F.G. Wilhelm, N.V.D. Vegt, M. Wessling, H. Strathmann, Bipolar membrane preparation, in: A. Kemperman (Ed.), Handbook of Bipolar Membrane Technology, 2000.
[30] Neosepta® Ion Exchange membranes, Product Brochure Tokuyama Soda Inc., Japan.

[31] J.-H. Choi, S.-H. Moon, Pore size characterization of cation-exchange membranes by chronopotentiometry using homologous amine ions, J. Membr. Sci. 191 (2001) 225–236.
[32] N. P Berezina, S.V. Timofeev, N.A. Kononenko, Effect of conditioning techniques of perfluorinated sulphocationic membranes on their hydrophylic and electrotransport properties, J. Membr. Sci. 209 (2002) 509–518.
[33] A. Chapotot, G. Pourcelly, G. Gavach, F. Lebon, Electrotransport of proton and divalent cations through modified cation exchange membranes, J. Electroanal. Chem. 386 (1995) 25–37.